

# Deep Learning-based Scatter Estimation for Time-of-Flight PET

Joscha Maier<sup>1</sup>, Yannick Berker<sup>3</sup>, Antje Schulte<sup>3</sup>, Maurizio Conti<sup>2</sup>,  
Jorge Cabello<sup>2</sup>, Deepak Bharkhada<sup>2</sup>, Antonis Kalemis<sup>3</sup>, Leyun Pan<sup>1</sup>,  
Antonia Dimitrakopoulou-Strauss<sup>1</sup>, and Marc Kachelrieß<sup>1</sup>

<sup>1</sup> German Cancer Research Center (DKFZ), Heidelberg, Germany

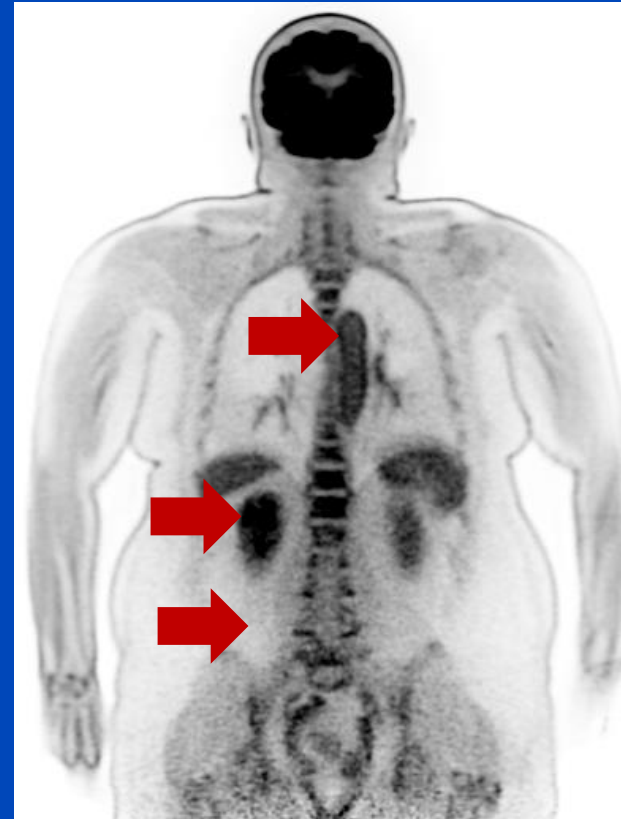
<sup>2</sup> Siemens Healthineers, Knoxville, Tennessee, USA

<sup>3</sup> Siemens Healthineers, Forchheim, Germany

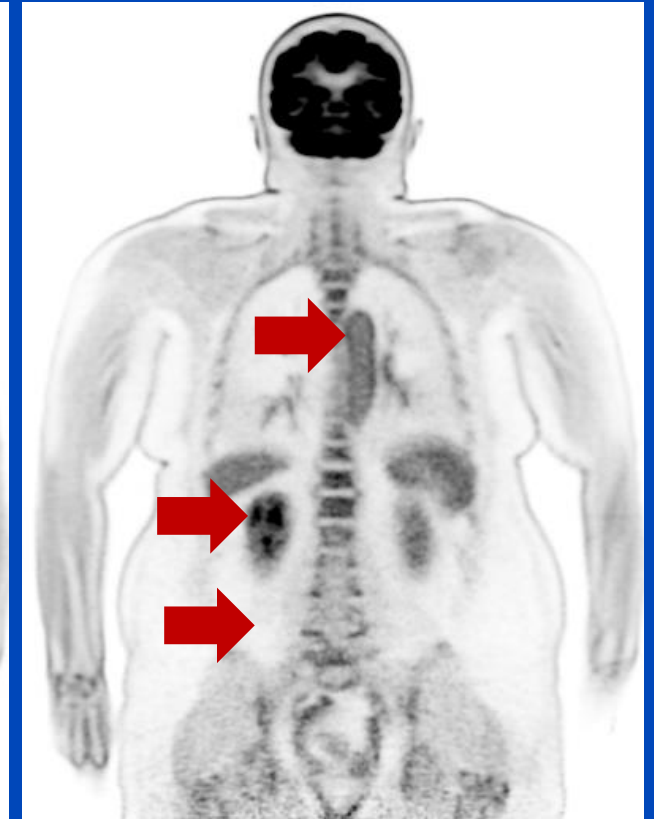
# Motivation

- Scatter is a major cause of image quality degradation in PET leading to:
  - Loss of contrast
  - Quantification bias
  - Image artifacts
- Scatter fraction in PET is often in the range of 30 - 40 %<sup>1,2,3,4</sup> for energies > ~420 keV.
- Precise scatter correction is crucial to maintain the diagnostic quality of the PET scan.

No scatter correction



MC scatter correction



[1] V. Bettinardi et al., "Physical performance of the new hybrid PET/CT discovery-690", *Med. Phys.* 38:5394–411, 2011

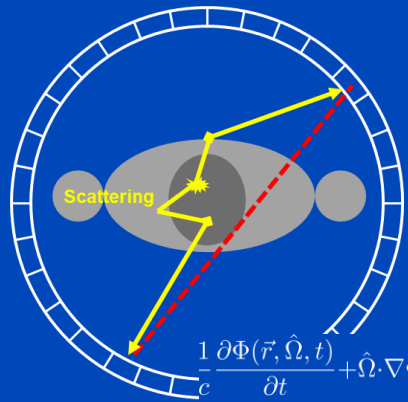
[2] S. Surti et al., "Performance of philips gemini TF PET/CT scanner with special consideration for its time-of-flight imaging capabilities", *J. Nucl. Med.* 48(3):471–80, 2007.

[3] J. van Sluis et al., "Performance characteristics of the digital biograph vision PET/CT system", *J. Nucl. Med.* 60(7):1031–6, 2019.

[4] B. Spencer B et al., "Performance evaluation of the EXPLORER total-body PET/CT scanner based on NEMA NU-2 2018 standard with additional tests for extended geometry", NSS/MIC 2019.

# Scatter Estimation / Correction: Prior Work

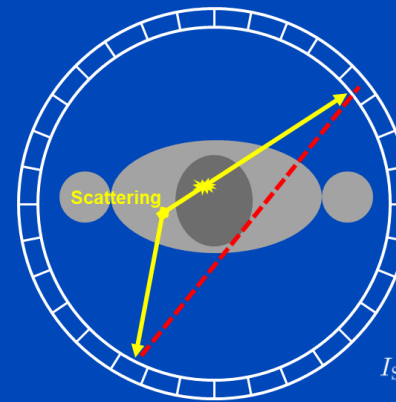
## Gold standard: Monte Carlo Simulation<sup>1</sup>



Numerical solution of the Boltzmann transport equation using physics-based random sampling.

$$\frac{1}{c} \frac{\partial \Phi(\vec{r}, \hat{\Omega}, t)}{\partial t} + \hat{\Omega} \cdot \nabla \Phi(\vec{r}, \hat{\Omega}, t) + \mu(\vec{r}, E) \Phi(\vec{r}, \hat{\Omega}, t) = \int_{4\pi} \frac{d\sigma(\hat{\Omega}' \rightarrow \hat{\Omega}, E)}{d\Omega} \Phi(\vec{r}, \hat{\Omega}', t) d\hat{\Omega}' + S(\vec{r}, \hat{\Omega}, t)$$

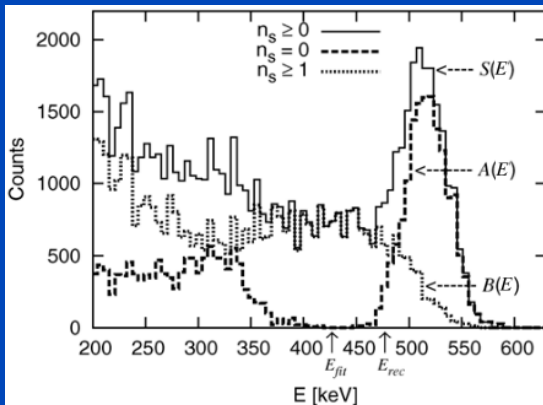
## Single Scatter Simulation<sup>2</sup>



Analytic solution of the Boltzmann transport equation using single scatter approximation.

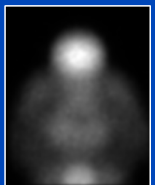
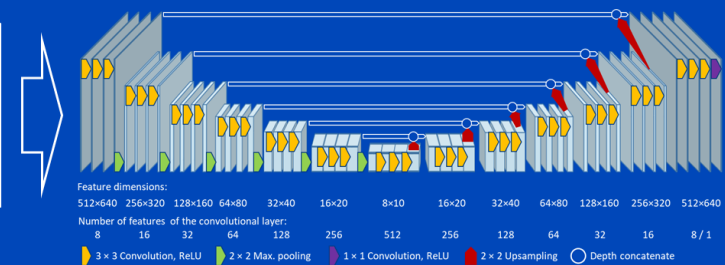
$$I_{SSS}(\vec{r}_1, \vec{r}_2) = I_0 \int_V d^3 r' T(\vec{r}_1, \vec{r}') T(\vec{r}_2, \vec{r}') \mu_s(\vec{r}') P(\hat{\Omega}'_1 \rightarrow \hat{\Omega}_1) P(\hat{\Omega}'_2 \rightarrow \hat{\Omega}_2)$$

## Energy-based Scatter Estimation<sup>3</sup>



Make use of the difference between the energy spectra of the unscattered and scattered photons.

## Deep Learning-based Scatter Estimation<sup>4</sup>



Train neural networks to correct for scatter / predict PET scatter distributions.

[1] H. Zaidi, "Relevance of accurate Monte Carlo modeling in nuclear medical imaging", *Med. Phys.* 26(4):574-608, 1999.

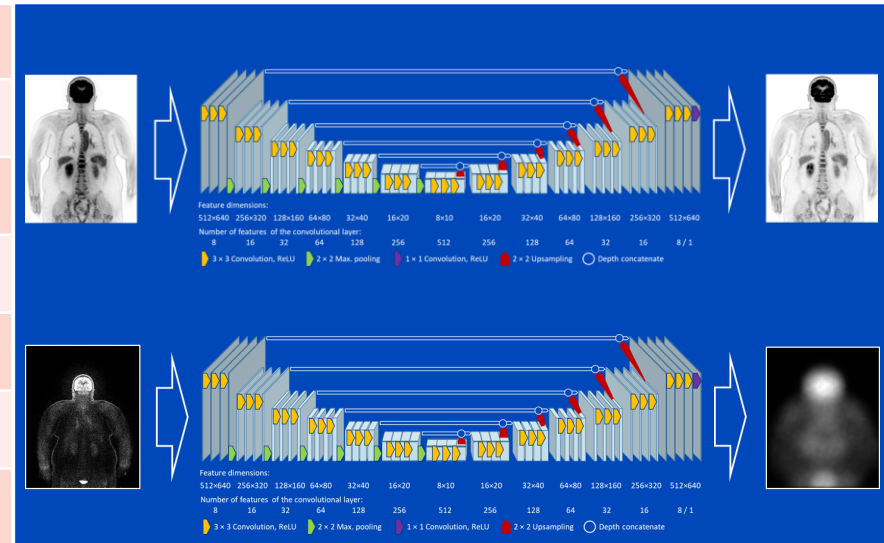
[2] J.M. Ollinger, "Model-based scatter correction for fully 3D PET", *Phys. Med. Biol.* 41(1), 153-176, 1996.

[3] L. M. Popescu et al. "PET energy-based scatter estimation and image reconstruction with energy-dependent corrections", *Phys. Med. Biol.* 51(11), 2919-2937, 2006.

[4] Y. Berker et al., "Deep Scatter Estimation in PET: Fast Scatter Correction Using a Convolutional Neural Network", NSS/MIC 2018.

# Deep Learning-based Scatter Estimation / Correction

Domain	#	TOF	Training / Application
Image	3	Yes	Uncorrected Reconstruction → Scatter-corrected reconstruction
	4	No	Uncorrected Reconstruction → Scatter-corrected reconstruction
	5	No	Uncorrected Reconstruction → Scatter-corrected reconstruction
	6	Yes	Monte Carlo correction based on DL Reconstruction
Sinogram	1	No	Single scatter → MC, emission/attenuation data → MC
	2	No	Emission/attenuation data → Single scatter
	7	No	Emission/attenuation data → MC scatter



[1] H. Qian et al., “Deep Learning Models for PET Scatter Estimations”, *NSS/MIC 2017*.  
 [2] Y. Berker et al., “Deep Scatter Estimation in PET: Fast Scatter Correction Using a Convolutional Neural Network”, *NSS/MIC 2018*.  
 [3] J. Yang et al., “Joint correction of attenuation and scatter in image space using deep convolutional neural networks for dedicated brain 18F-FDG PET”, *Phys. Med. Biol.* 64(7), 2019.  
 [4] I. Shiri et al., “Deep-JASC: joint attenuation and scatter correction in whole-body 18F-FDG PET using a deep residual network”. *EJNMMI* 47(11), 2533–2548, 2020.  
 [5] S. Mostafapour et al., “Feasibility of Deep Learning-Guided Attenuation and Scatter Correction of Whole-Body 68Ga-PSMA PET Studies in the Image Domain”, *Clin. Nucl. Med.* 46(8), 609–615, 2021  
 [6] K. Li et al., “Deep Learning Accelerates Accurate Scatter Correction with Histo-image in TOF PET/CT System”, *NSS/MIC 2022*  
 [7] B. Laurent et al., “PET scatter estimation using deep learning U-Net architecture”, *Phys. Med. Biol.* 68(6), 2023.

# Sinogram Domain Scatter Estimation

## What's New in this Work?

- **Deep scatter estimation (DSE) for TOF PET scans:**
  - Can DSE be generalized to different TOF bins?
  - Is there an advantage of processing all TOF bins simultaneously?
- **Application to long axial FOV PET scanner:**
  - Can DSE be generalized to highly oblique planes?



Whole-body TOF PET system.

# Data Generation: Monte Carlo Simulation

Siemens Biograph  
Vision Quadra  
@ DKFZ

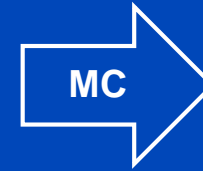


Whole-body TOF  
scans with two bed  
positions

Initial PET  
reconstruction +  
SSS



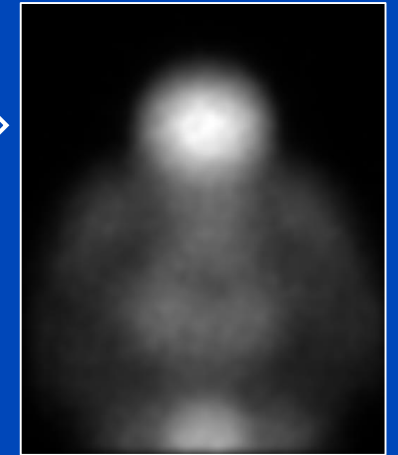
CT  
attenuation  
map



List  
mode  
data



MC Scatter  
distribution



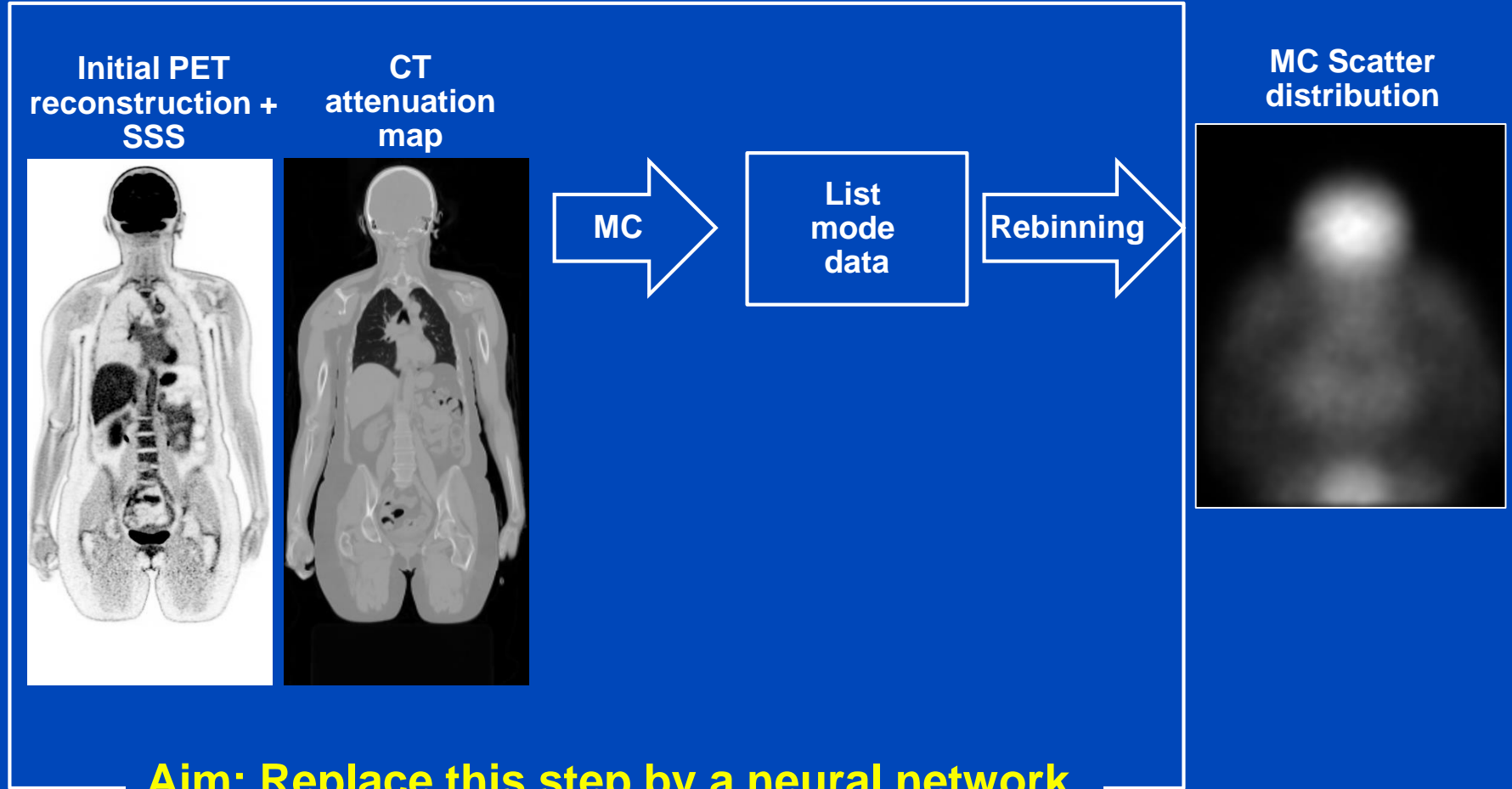


# Data Generation: Monte Carlo Simulation

Siemens Biograph  
Vision Quadra  
@ DKFZ

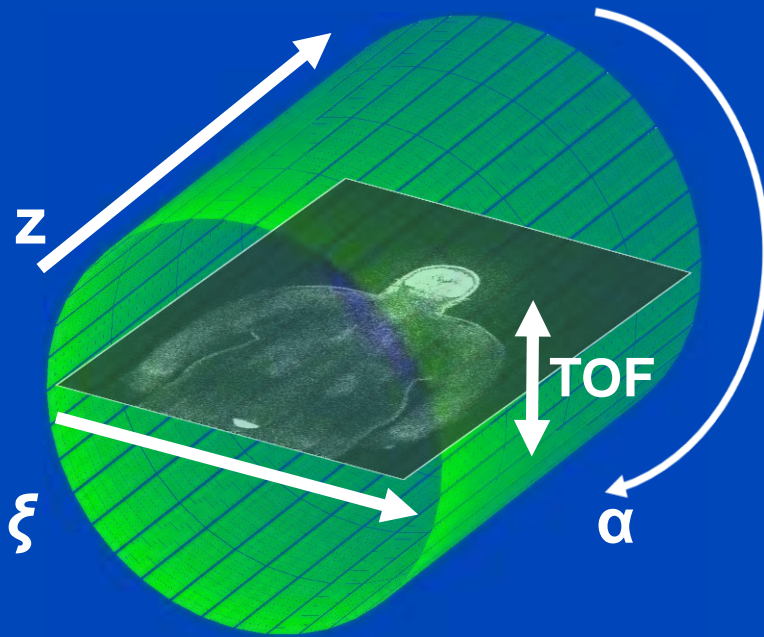


Whole-body TOF  
scans with two bed  
positions



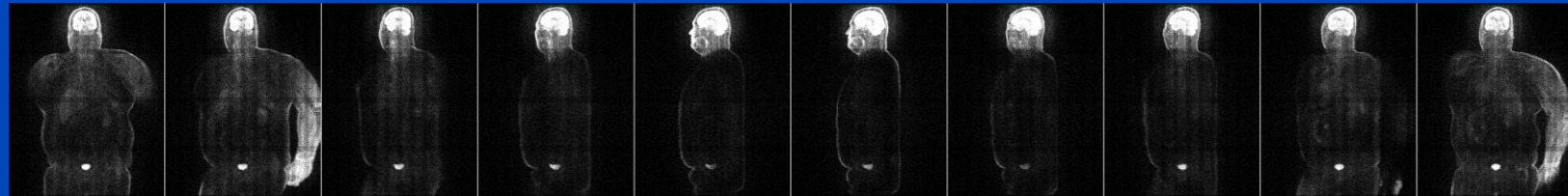
# Data Representation

## Emission data

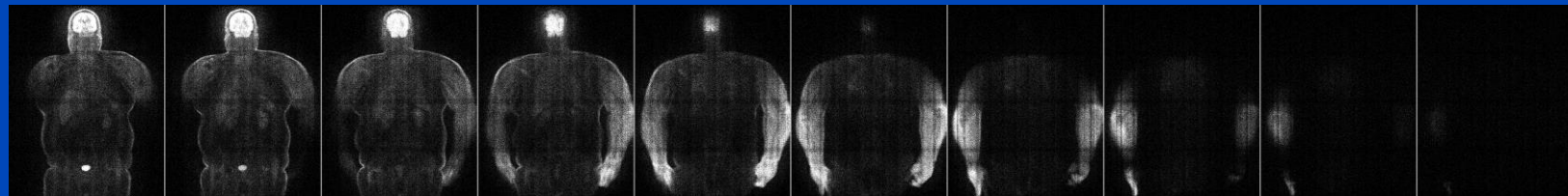


- All experiments shown in the following use 2D sub-sinograms in  $\xi$ -z-plane, i.e. for each plane we have:

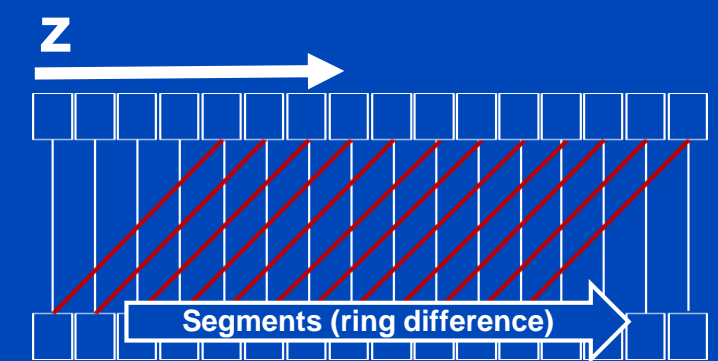
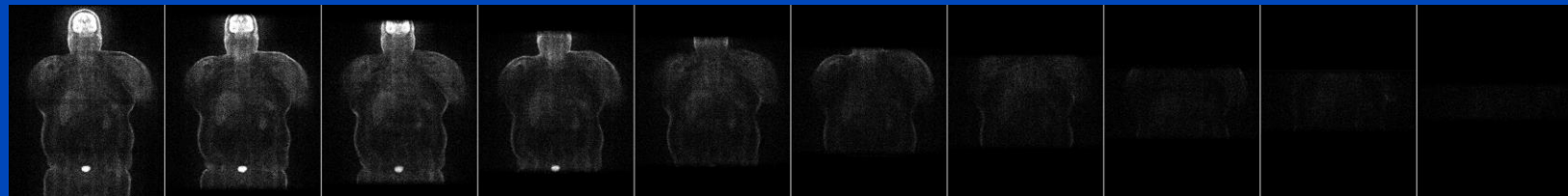
50 angles,  $0^\circ$ - $180^\circ$ ,  $\Delta\alpha = 3.6^\circ$  (not all angles shown)



33 TOF bins,  $\Delta\text{TOF} = 143$  ps (not all TOF bins shown)



35 segments, Max. ring diff. = 322, axial compr. = 19 (not all shown)

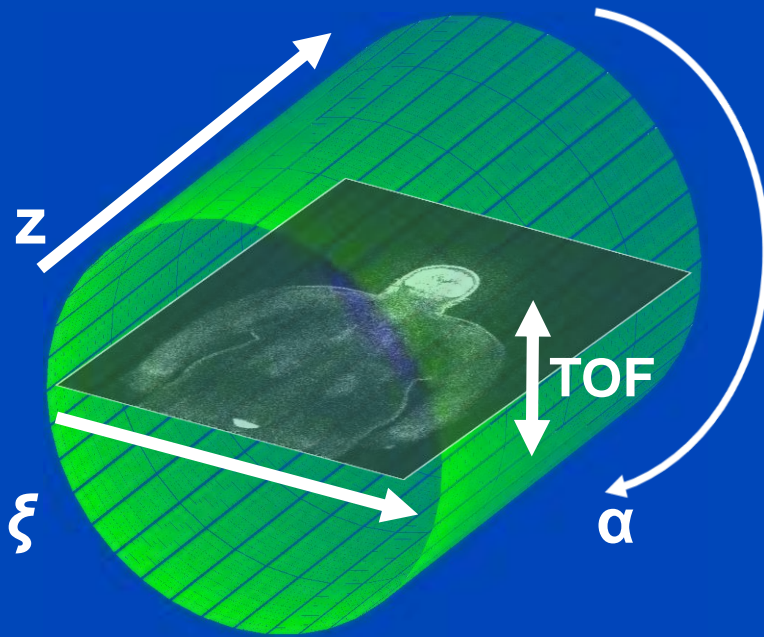


→ 57750  $\xi$ -z-planes / scan



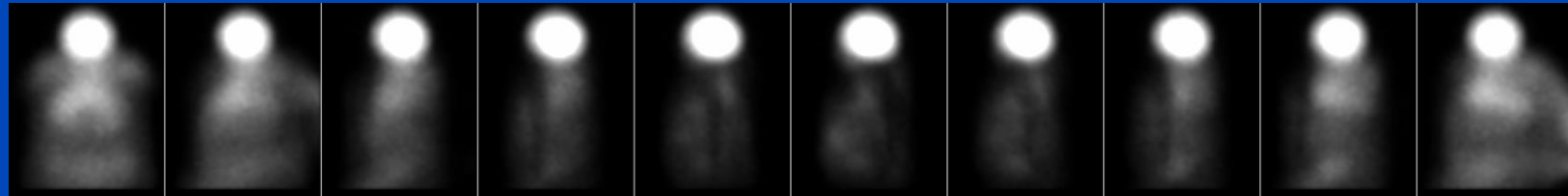
# Data Representation

## Scatter distributions

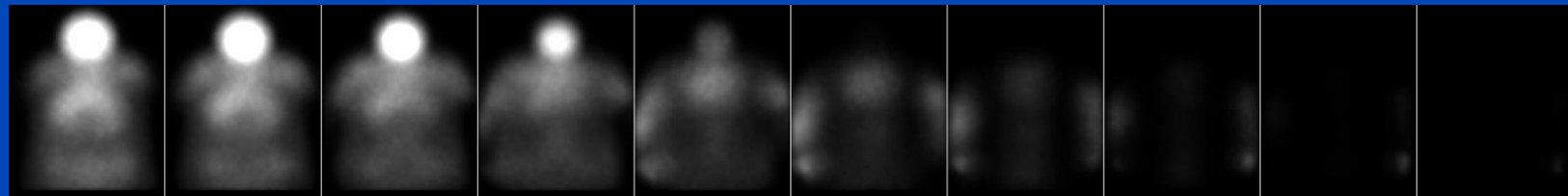


- All experiments shown in the following use 2D sub-sinograms in  $\xi$ -z-plane, i.e. for each plane we have:

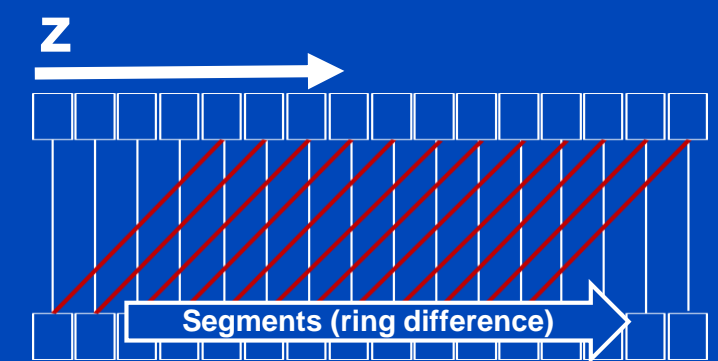
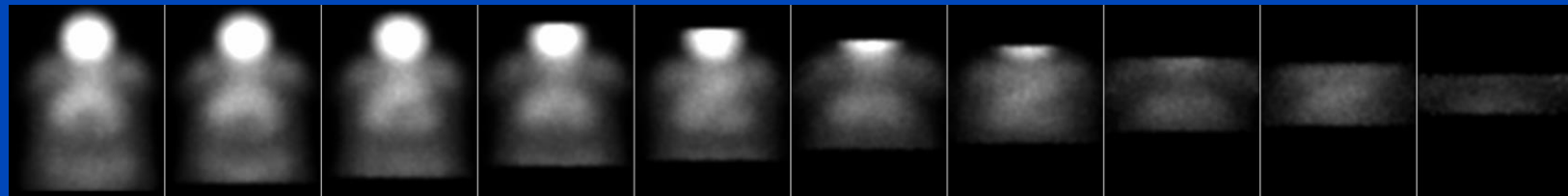
50 angles,  $0^\circ$ - $180^\circ$ ,  $\Delta\alpha = 3.6^\circ$  (not all angles shown)



33 TOF bins,  $\Delta\text{TOF} = 143$  ps (not all TOF bins shown)



35 segments, Max. ring diff. = 322, axial compr. = 19 (not all shown)

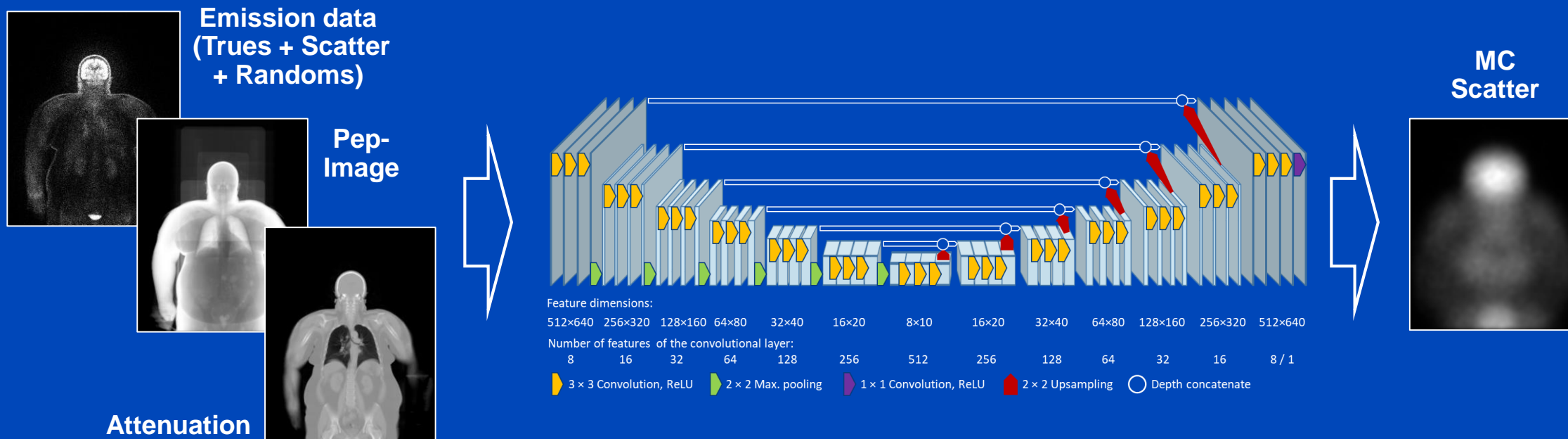


→ 57750  $\xi$ -z-planes / scan

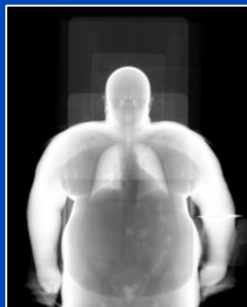
# PET Deep Scatter Estimation

Realization #1: Each TOF bin as separate input

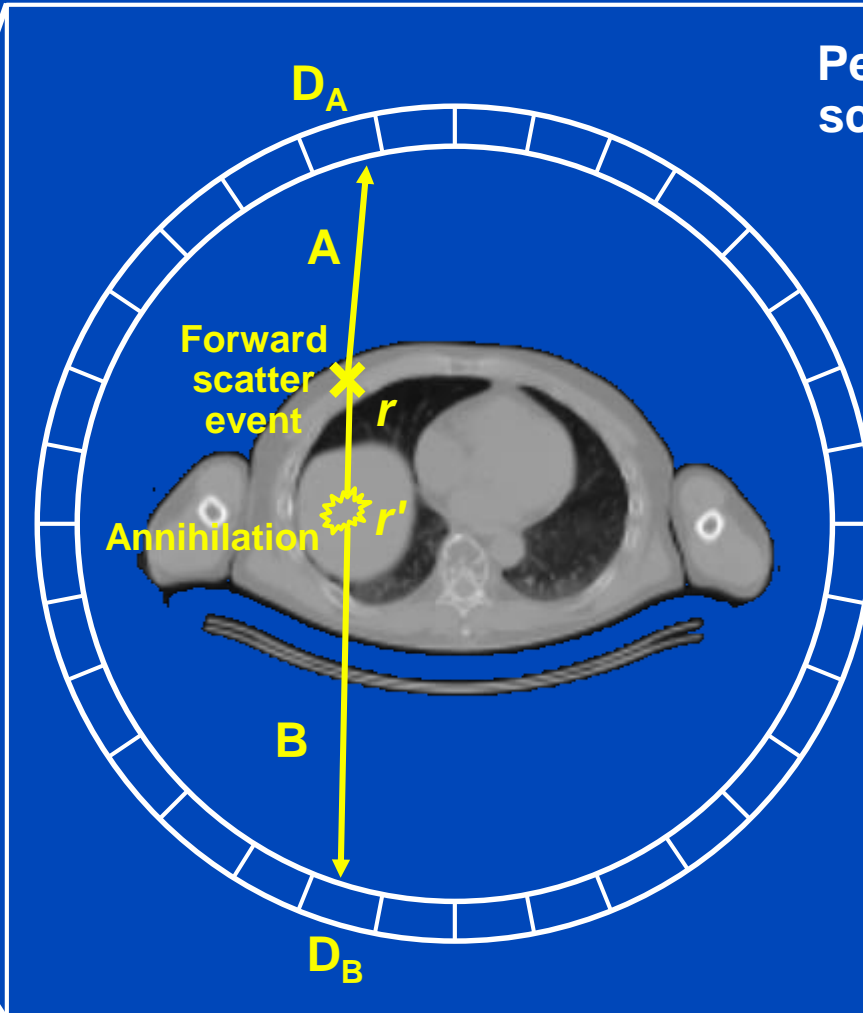
- Use measured activity (trues + scatter + randoms), pep-image, and attenuation image as 3-channel input to a U-net.
- Minimize MSE between prediction and the MC to optimize the network's weights
- Training on 50 patients / Testing on 6 patients.



# Pep-Image



Pep-Image<sup>1</sup>



**Pep = Approximation of single-scattering in forward direction.**

$$\begin{aligned} \text{Pep} = & \text{Activity } A(r') \text{ at } r' \\ & \times \int \text{Probability of A being scattered} \\ & \times \text{Probability scattered A reaching } D_A \\ & \times \text{Probability of B reaching } D_B \, dr \\ = & A(r') \cdot p \cdot e^{-p} \end{aligned}$$

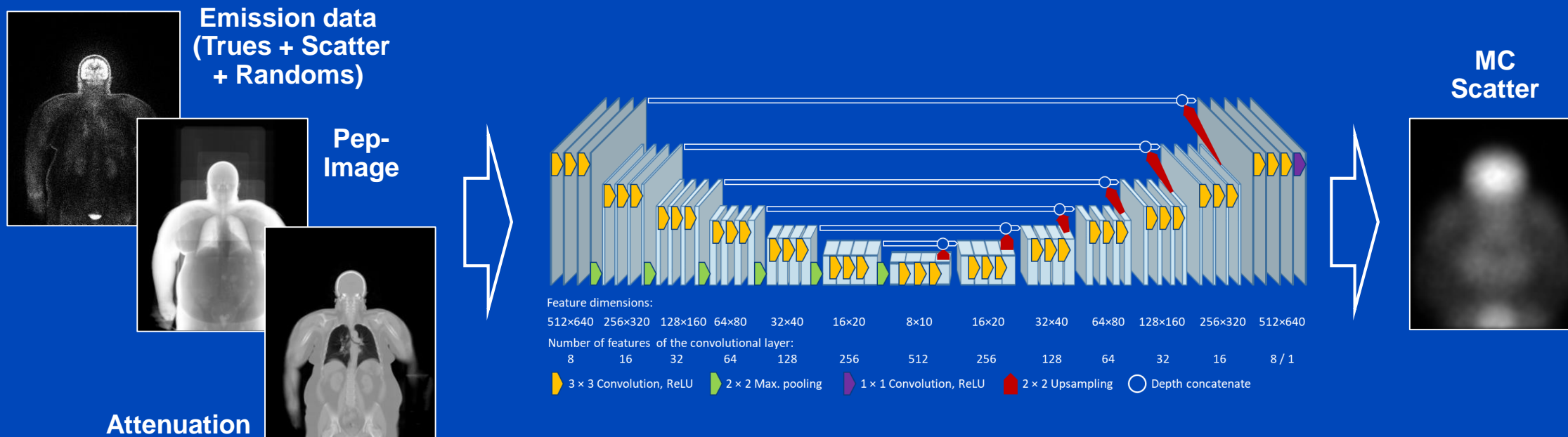
with

$$p = \int_{D_A}^{D_B} \mu(r) dr$$

# PET Deep Scatter Estimation

Realization #1: Each TOF bin as separate input

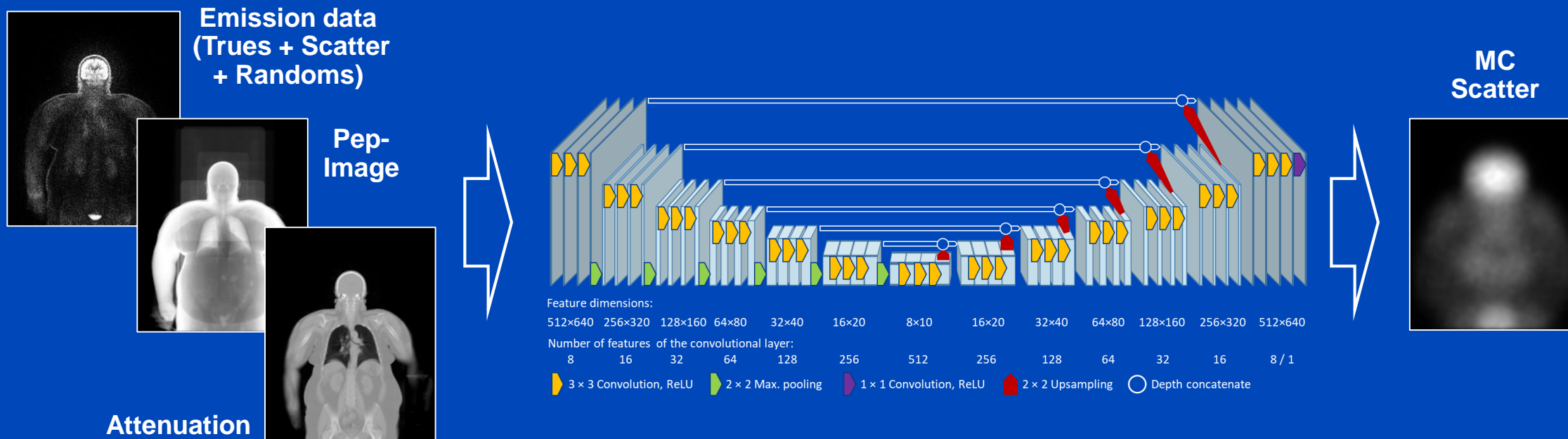
- Use measured activity (trues + scatter + randoms), pep-image, and attenuation image as 3-channel input to a U-net.
- Minimize MSE between prediction and the MC to optimize the network's weights
- Training on 50 patients / Testing on 6 patients.



# PET Deep Scatter Estimation

Realization #1: Each TOF bin as separate input

- Use measured activity (trues + scatter + randoms), pep-image, and attenuation image as 3-channel input to a U-net.
- Minimize MSE between prediction and the MC to optimize the network's weights
- Training on 50 patients / Testing on 6 patients.

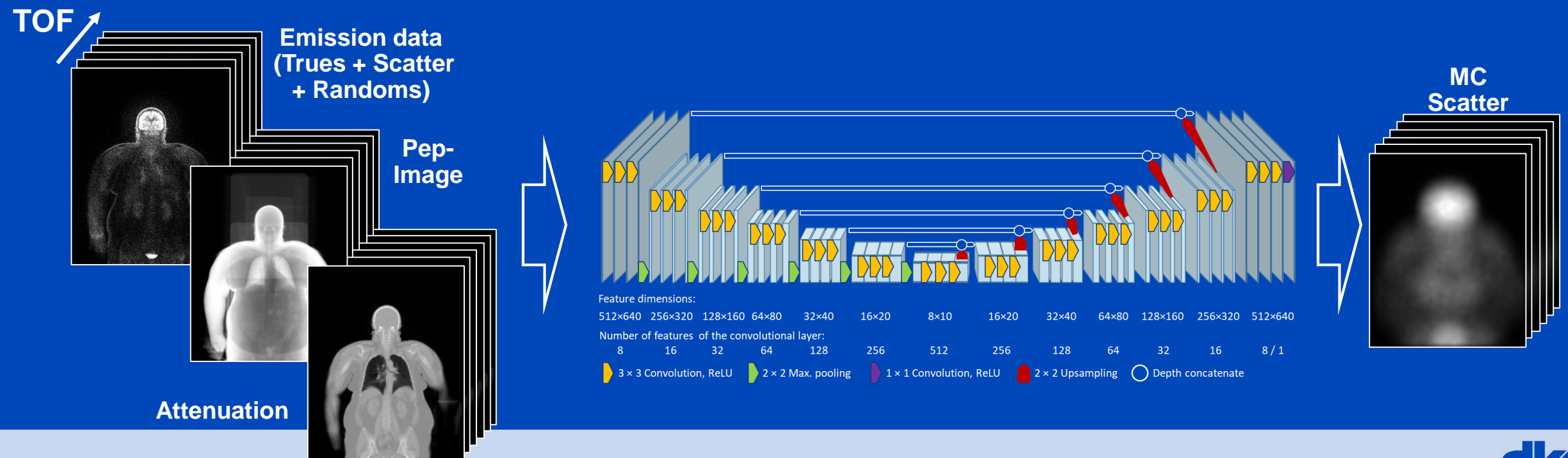




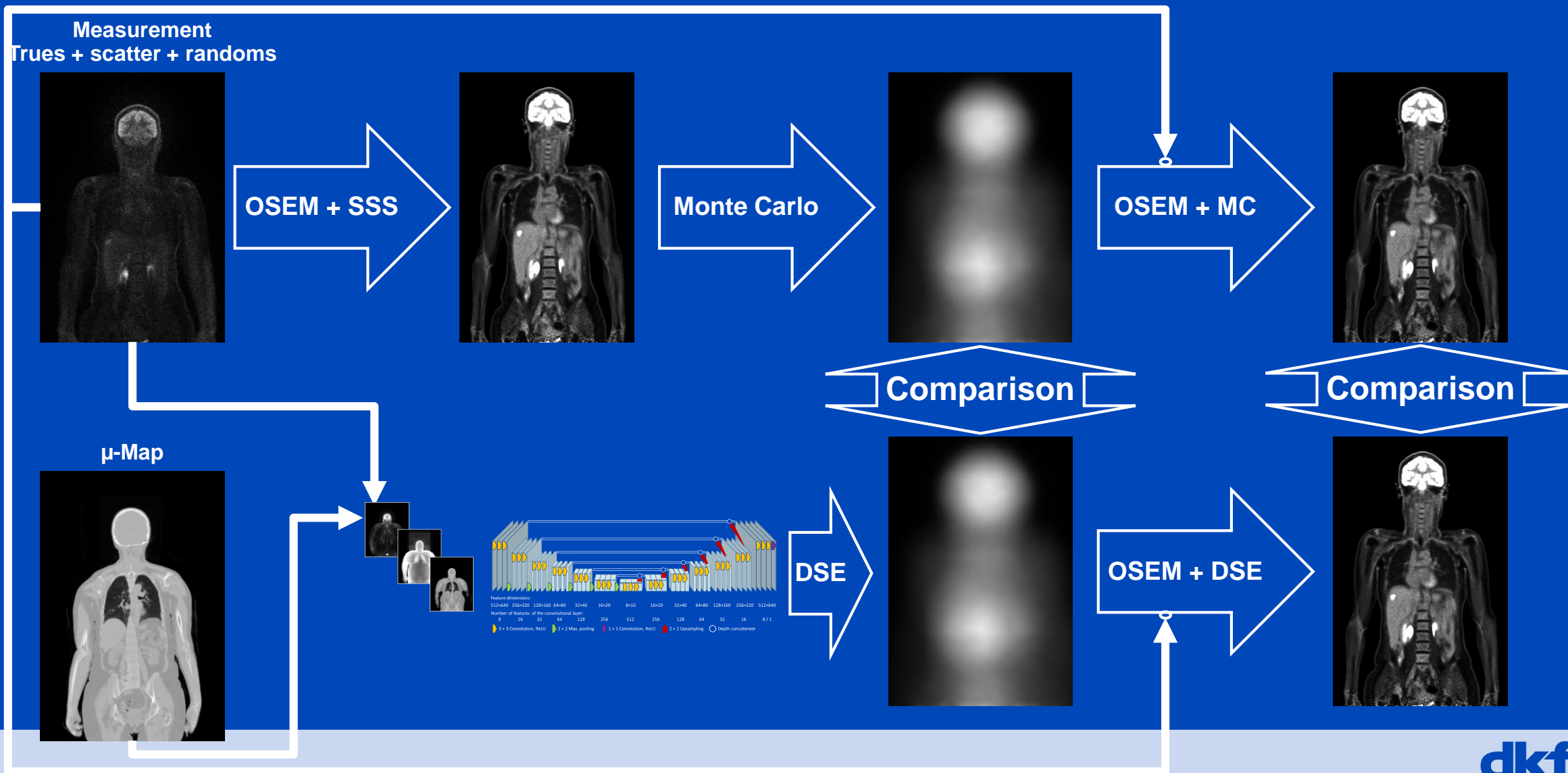
# PET Deep Scatter Estimation

## Realization #2: All TOF bins as multi-channel input

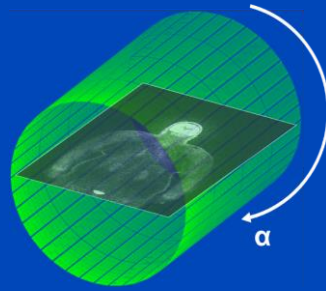
- Use measured activity (trues + scatter + randoms), pep-image, and attenuation of all TOF bins as multi-channel input.
- Minimize MSE between prediction and the MC to optimize the network's weights
- Training on 50 patients / Testing on 6 patients.



# DSE Testing (6 Patients)



# Results: TOF-bin 0, Segment 0, Angles 0 - 49



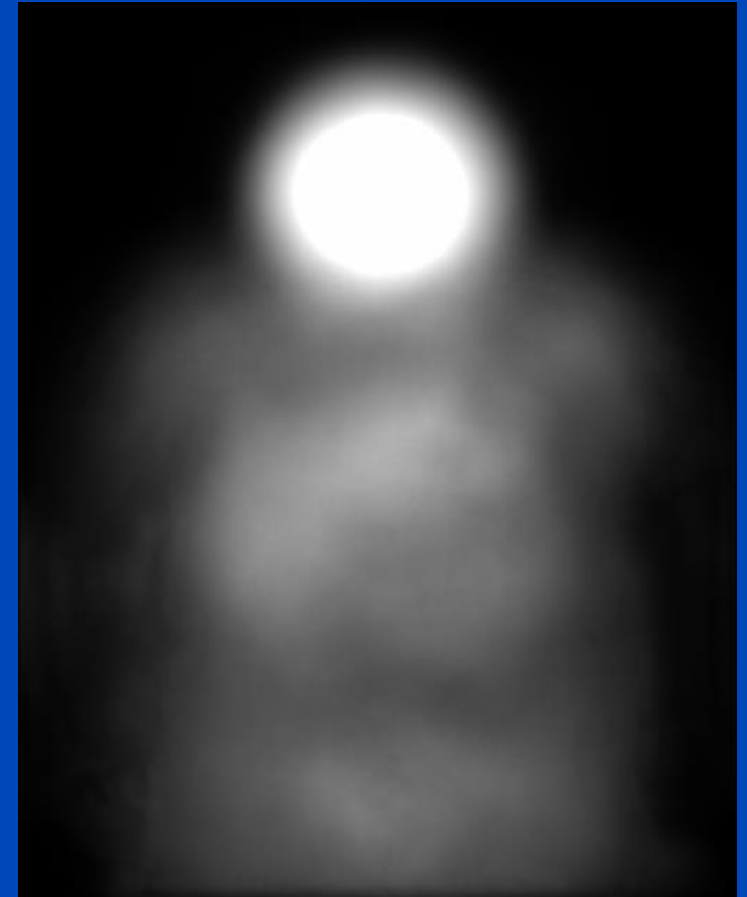
Monte Carlo Simulation



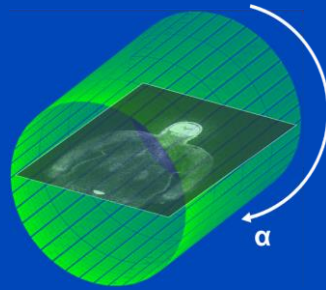
DSE #1 (single inputs)



DSE #2 (all TOF)



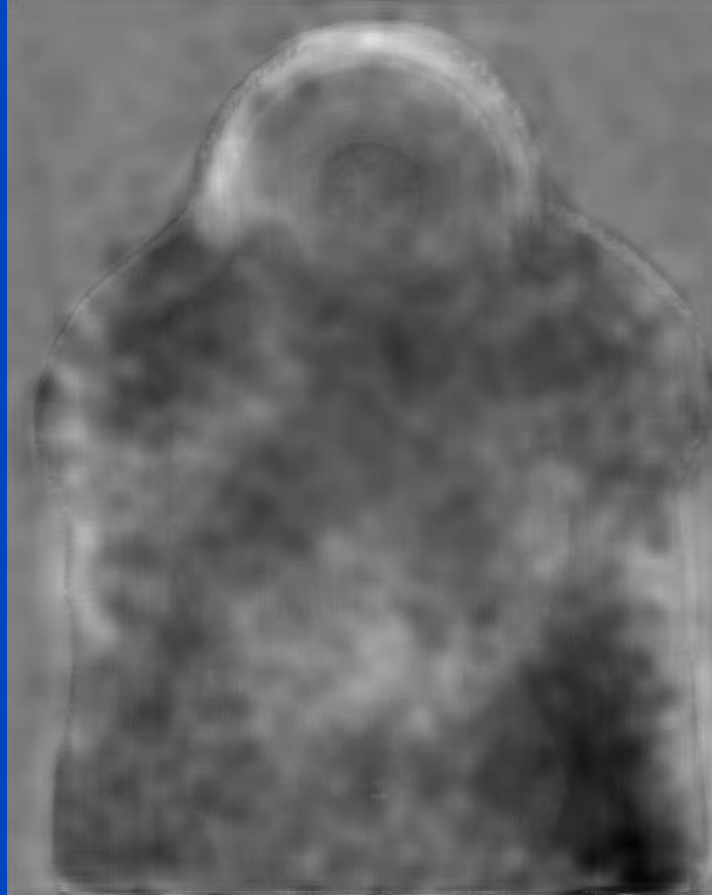
# Results: TOF-bin 0, Segment 0, Angles 0 - 49



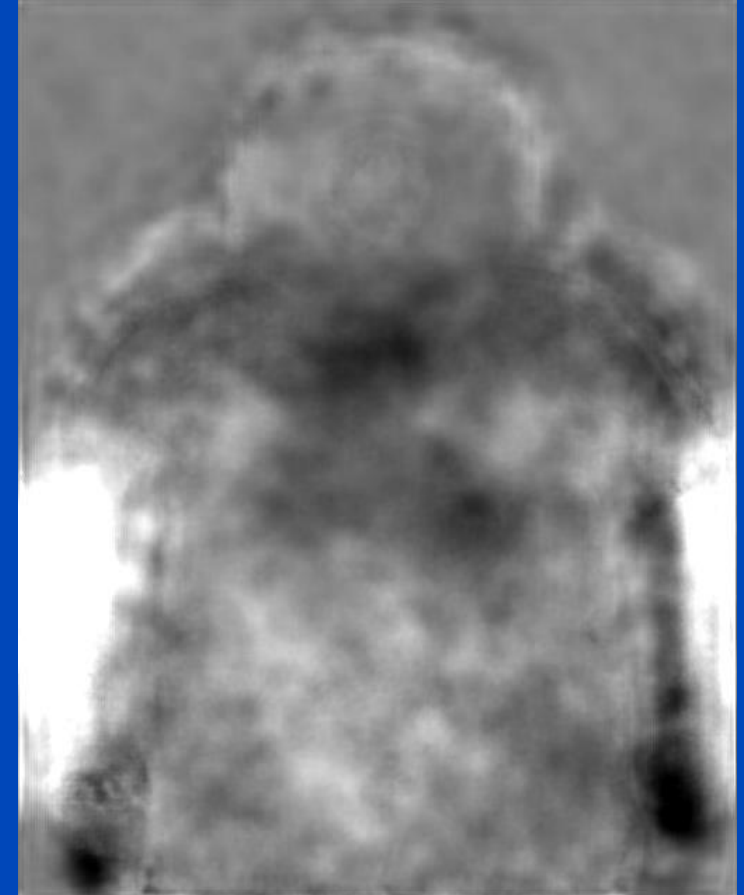
Monte Carlo Simulation



Relative error DSE #1

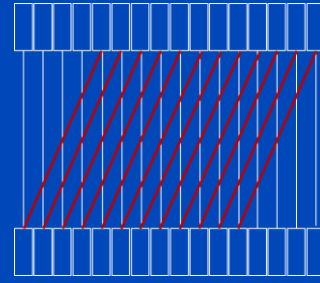


Relative error DSE #2



C = 0 %, W = 60 %

# Results: TOF-bin 0, Segments 0 - 34, Angle 0



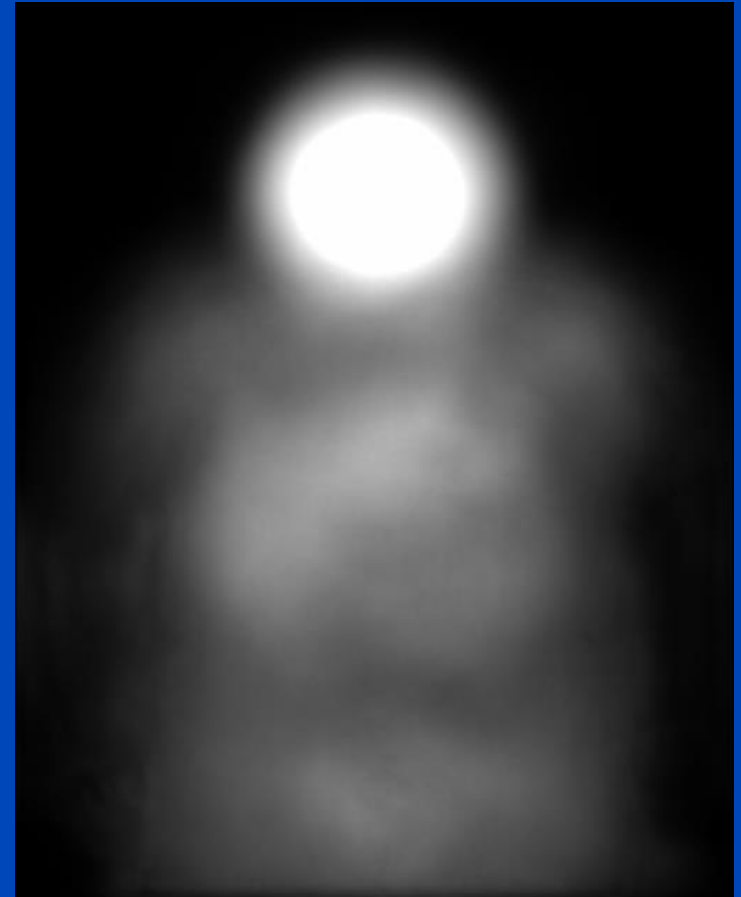
Monte Carlo Simulation



DSE #1 (single inputs)

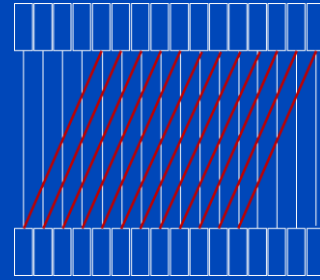


DSE #2 (all TOF)





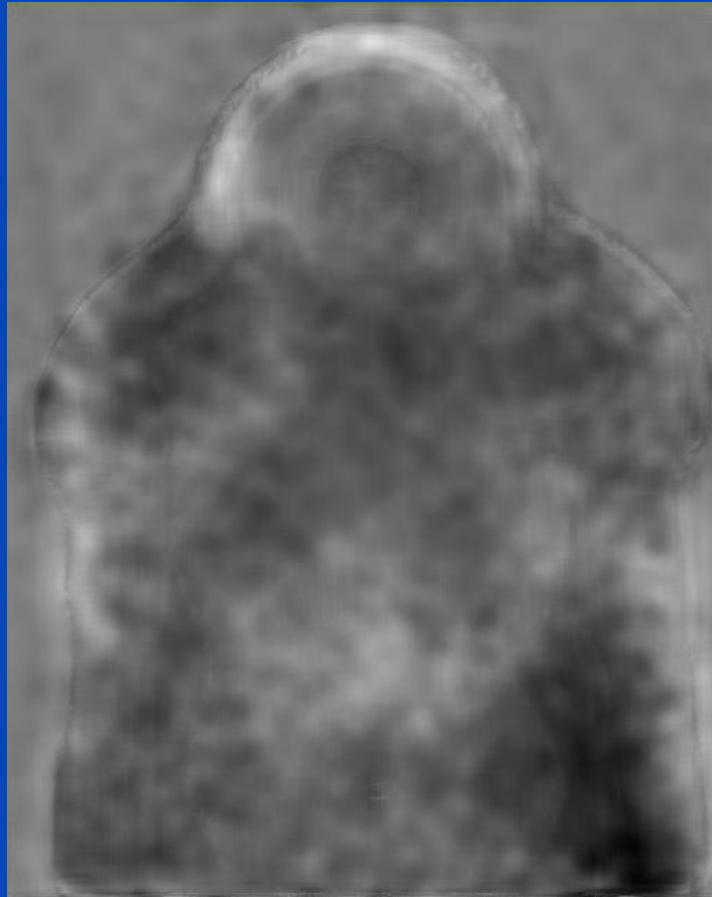
# Results: TOF-bin 0, Segments 0 - 34, Angle 0



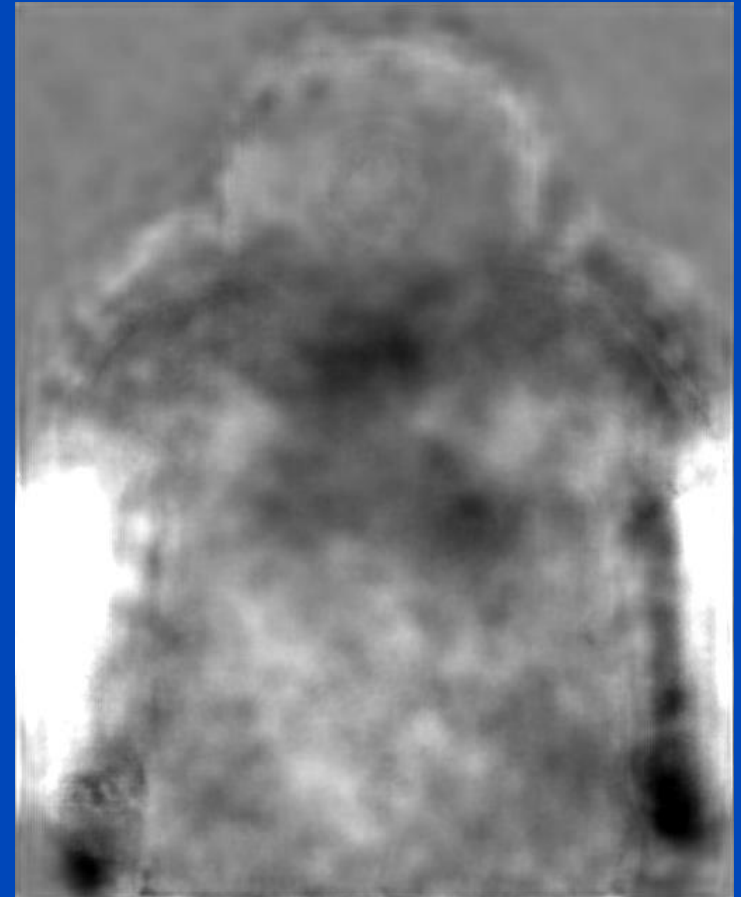
Monte Carlo Simulation



Relative error DSE #1

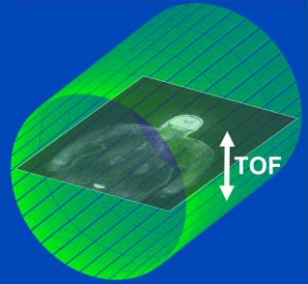


Relative error DSE #2

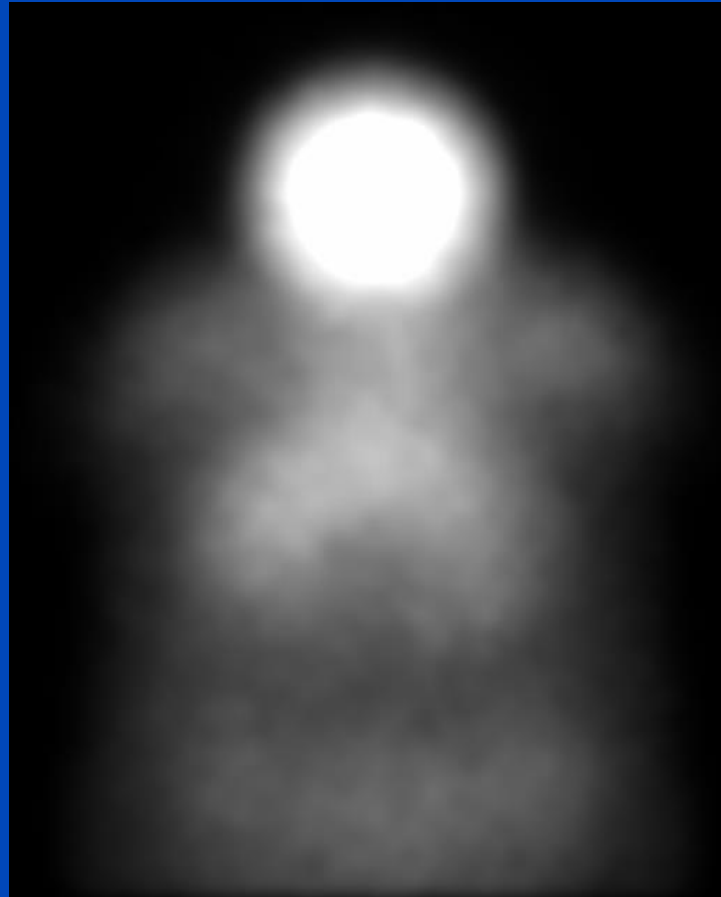


C = 0 %, W = 60 %

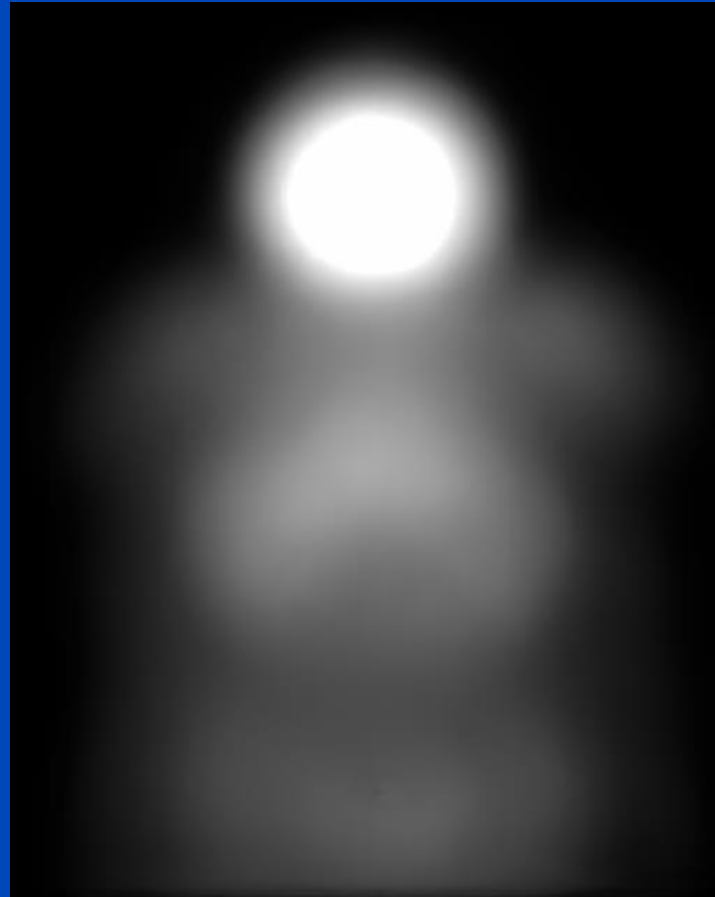
# Results: TOF-bins 0 - 32, Segment 0, Angle 0



Monte Carlo Simulation



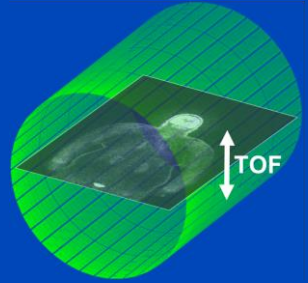
DSE #1 (single inputs)



DSE #2 (all TOF)



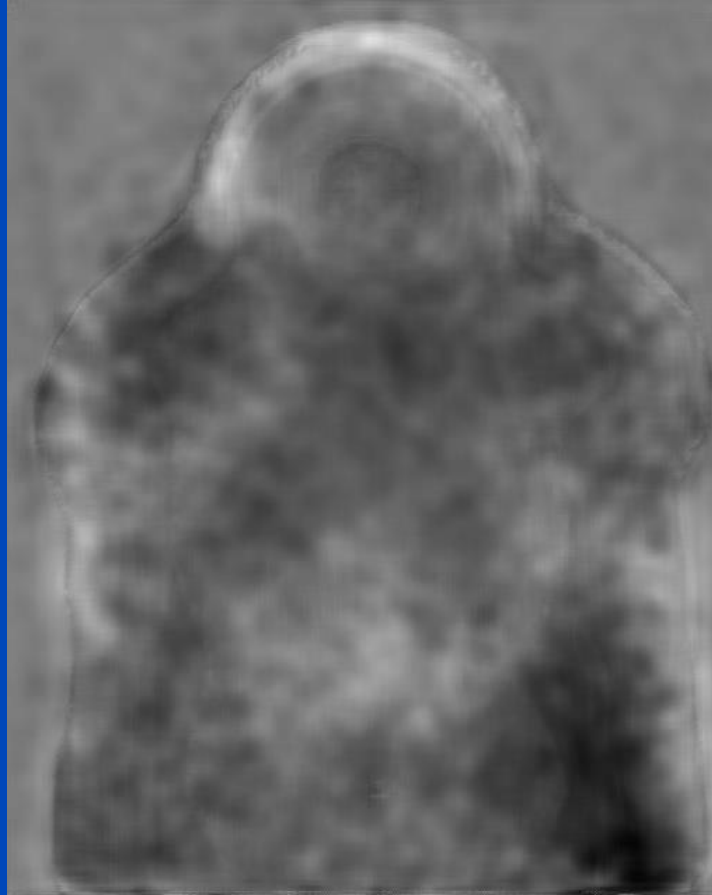
# Results: TOF-bins 0 - 32, Segment 0, Angle 0



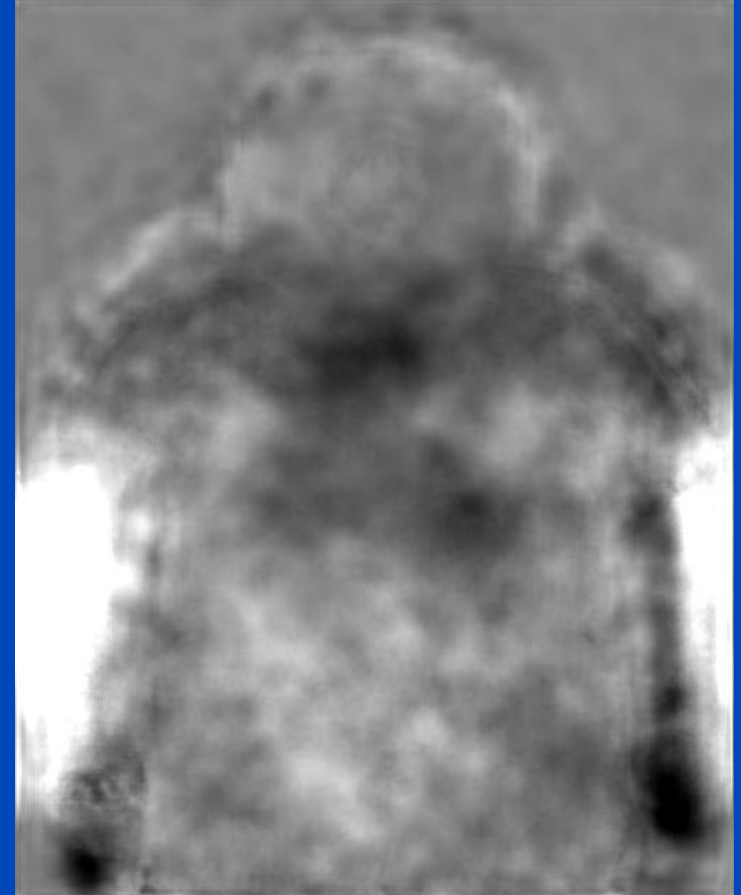
Monte Carlo Simulation



Relative error DSE #1

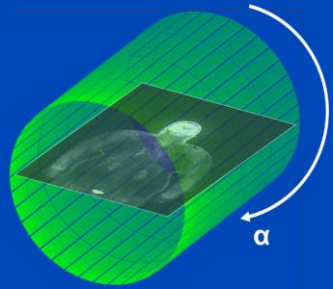


Relative error DSE #2

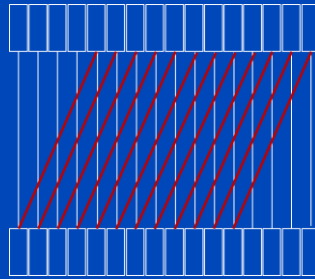


C = 0 %, W = 60 %

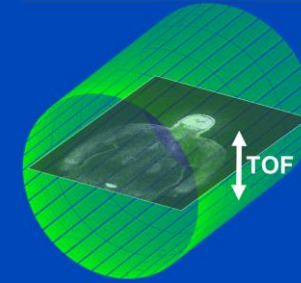
# Evaluation for All Test Patients – Mean Absolute Percentage Error of Scatter Estimates



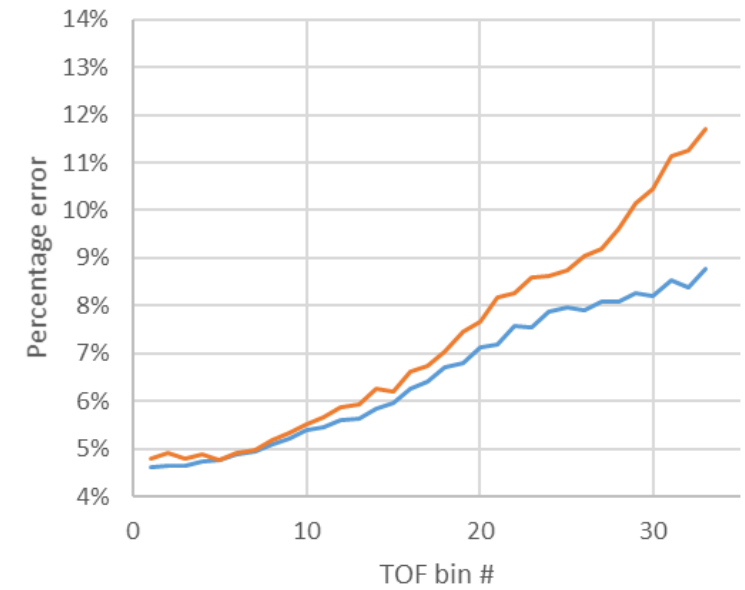
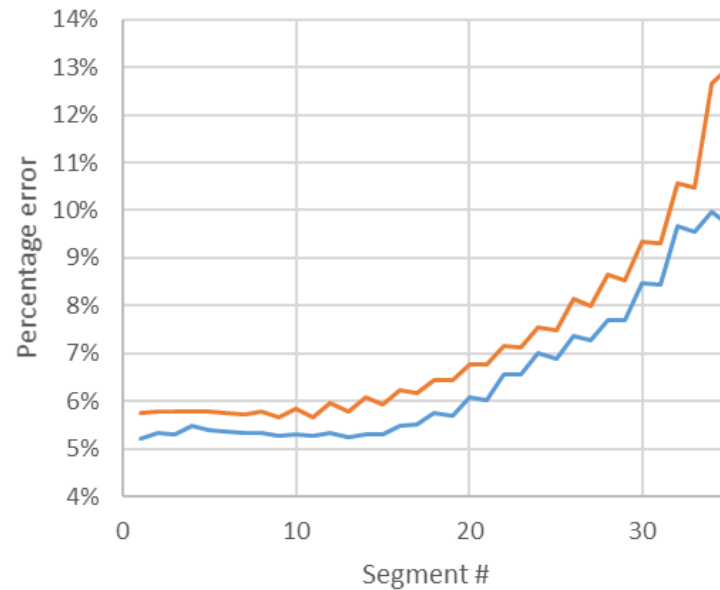
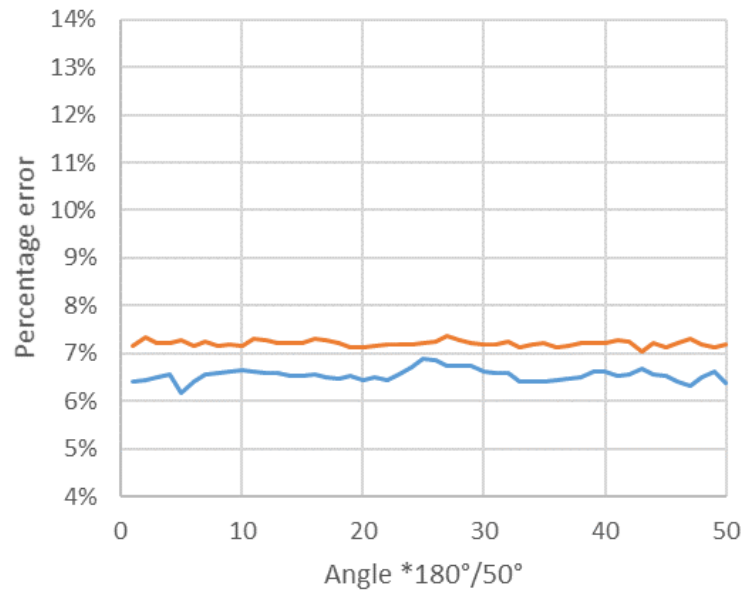
Angular dependence



Segment dependence



TOF bin dependence



— Single TOF bin

— All TOF bins as channels

# PET Reconstructions + Scatter Correction

Female patient, BMI = 43

No Correction



Monte Carlo (MC)



Siemens SSS



DSE #1



DSE #2



C = 2000, W = 4000



# PET Reconstructions + Scatter Correction

Female patient, BMI = 43

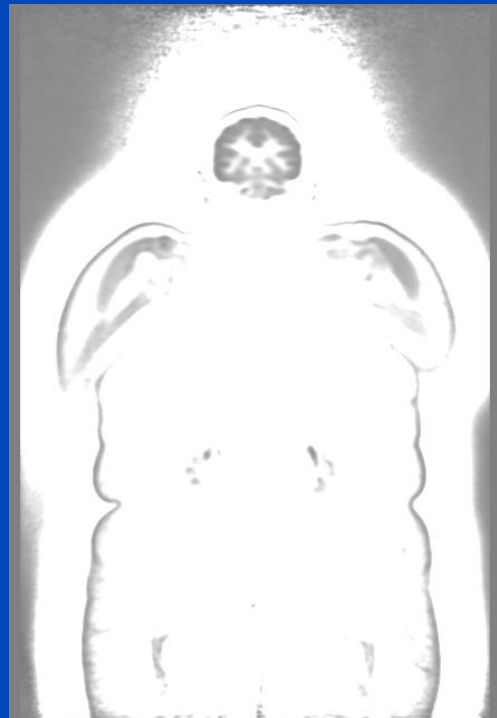
(No Correction – MC)/MC

Monte Carlo (MC)

(Siemens SSS – MC)/MC

(DSE #1 – MC)/MC

(DSE #2 – MC)/MC



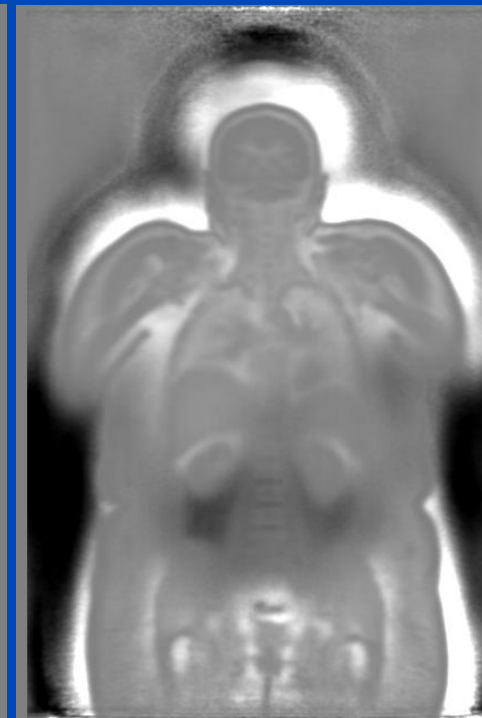
Avg: 140.7 %



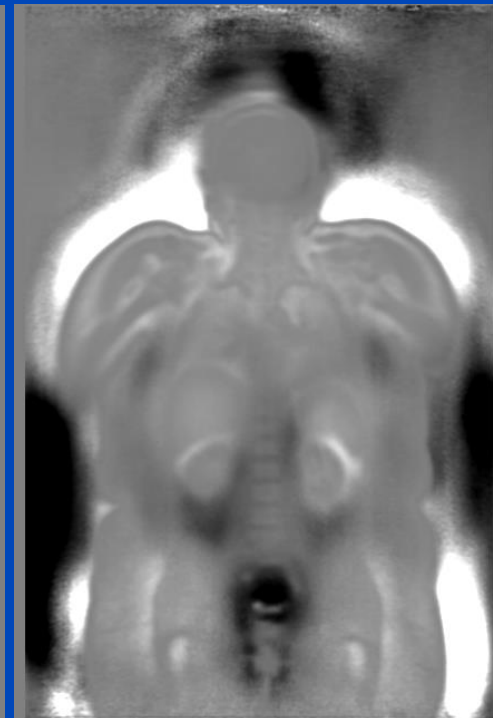
Avg: 27.8 %



Avg: 6.5 %



Avg: 7.1 %



C = 0 %, W = 100 %

# Conclusions

- DSE can reproduce Monte Carlo Scatter estimates with a mean absolute percentage error (MAPE) of about 6 % (SSS error: 23 %).
- Similar trends are observed for scatter-corrected reconstructions with a MAPE of 7 % for DSE and a MAPE of 28 % for SSS.
- A single DSE network can be trained to account for different TOF bins and different segments, however, with a slightly reduced accuracy for higher TOF values and highly oblique planes.
- No advantage of processing all TOF bins at once as different input channels to the network.
- Runtime: 5 ms per sample (520 x 645), 5 min per data set (~ runtime of SSS).

# Thank You!

This presentation will soon be available at [www.dkfz.de/ct](http://www.dkfz.de/ct)

Job opportunities through DKFZ's international PhD or Postdoctoral Fellowship programs ([www.dkfz.de](http://www.dkfz.de)), or directly through Prof. Dr. Marc Kachelrieß ([marc.kachelriess@dkfz.de](mailto:marc.kachelriess@dkfz.de)).

Parts of the reconstruction software were provided by RayConStruct® GmbH, Nürnberg, Germany.